Development of the Sensitizer for Generating Higher-Energy Photons under Diluted Condition via the Triplet-Triplet Annihilation-Supported Upconversion

Kazuo Tanaka, Wataru Ohashi, Kenichi Inafuku, Shohei Shiotsu, Yoshiki Chujo*

Department of Polymer Chemistry, Graduate School of Engineering, Kyoto University,

Katsura, Nishikyo-ku, Kyoto 615-8510, Japan

E-mail: tanaka@poly.synchem.kyoto-u.ac.jp

Phone: +81-75-383-2604

Fax: +81-75-383-2605

KEY WORDS: upconversion, triplet-triplet annihilation, sensitizer

ABSTRACT

It was previously reported that photon upconversion can occur in the solution containing anthracene and the Pt complex of octaethylporphyrin (PtOEP) via the triplet-triplet annihilation process. In this study, by employing the modified Pt complex of the dual anthracene-tethered porphyrin, DA-PtP as a sensitizer, it is demonstrated that shorter-wavelength light can be generated under diluted condition. We synthesized DA-PtP and compared upconversion properties by changing the type of sensitizers. Accordingly, it was shown that the photon upconversion proceeded with the xenon lamp (540 nm) in the presence of DA-PtP. Furthermore, it was found that the emission band in the shorter wavelength light in the near UV region was observed from the solution containing DA-PtP even under diluted condition. From the mechanistic investigation, it was proposed that the anthracene moieties in DA-PtP might inhibit to form agglomeration with the free anthracene. As a result, reabsorption of the higher-energy light generated from upconversion could be suppressed.

INTRODUCTION

The developments of new photo-cleavable functional groups and photoactivated prodrugs are of significance in photo-medical treatments.[1–3] However, intrinsic low permeability of the light near 400 nm in the vital body is still the critical limitation on the application of activation to these photo-responsive drugs at the deep spot inside bodies. One of potential strategies for overcoming this problem is to combine the photon upconversion, in which the lower-energy incident light can be converted to the higher-energy light.[4,5] In ideal, by co-adding the photoactivated prodrugs with the anti-Stokes materials which can cause upconversion, the permeable lower-energy light can be used for the activation of the photoactivated prodrugs without significant decay of the incident light and damages to the bodies. Thus, the photon upconversion is promised to be a key technology for extending the applicability of the photomedical treatments.

When two triplet-excited molecules encounters, the one singlet-excited molecule can be generated from two triplet-excited molecules. This phenomenon is called as triplet-triplet annihilation (TTA, Scheme 1).[6–9] By selecting the types of sensitizers and emitters, the wavelengths of the acceptable incident and the generated light can be tuned.[6–9] Indeed, TTA-supported upconversion systems have been applied for *in vivo* imaging.[10–16] In particular, since UV light, which is favourable for inducing photo-activation into prodrugs, can be generated, TTA-supported upconversion is regarded as a promising tool for realizing phototherapy inside bodies.[17–20] However, another critical issue must be considered under biological conditions. In our previous reports, the related molecules were loaded onto the dendrimers having the silica element-block[21,22] for facilitating efficient energy transferring and TTA.[23,24] It is likely that the local concentrations of sensitizers and fluorophores would decrease due to diffusion, while the upconversion efficiency strongly depends on the concentration of the triplet-excited molecules. To overcome this problem, the new system should be required for obtaining higher efficiency even under diluted conditions.

Scheme 1

Herein, we report the TTA-supported upconversion for receiving higher-energy light than those from conventional systems by employing the modified Pt porphyrin complex having the dual anthracene substituents, DA-PtP, as a triplet sensitizer. From the comparison of upconversion emission with DA-PtP and the conventional Pt porphyrin (platinum octaethylporphyrin, PtOEP), it was observed that the upconversion with a larger energy gap can be observed under diluted conditions with the xenon lamp as a light source in the presence of DA-PtP. From the series of experiments, it was suggested that the anthracene moieties in DA-PtP might inhibit to form agglomeration with the free anthracene. As a result, reabsorption of the higher-energy light generated from upconversion could be suppressed. The upconversion system was obtained for generating higher-energy light with the smaller amounts of a sensitizer and an emitter than those in conventional systems.

Experimental

General. ^{1}H NMR and ^{13}C NMR spectra were measured with a JEOL EX-400 (400 MHz for ^{1}H and 100 MHz for ^{13}C) spectrometer. Coupling constants (*J* value) are reported in Hertz. The chemical shifts are expressed in ppm downfield from tetramethylsilane, using residual chloroform (δ = 7.24 in ^{1}H NMR, δ = 77.0 in ^{13}C NMR) as an internal standard. Column chromatography was performed with Wakogel C-300 silica gel. UV–vis absorption spectra were obtained at 25 °C using 1 cm path length cell with a SHIMADZU UV-3600UV-vis-NIR spectrophotometer. The fluorescence emission under excitation at 540 nm was monitored using a Perkin Elmer LS50B at 25 °C using 1 cm path length cell with a 480-nm cut-off filter. The excitation bandwidth was 15 nm. The emission bandwidth was 5 nm. Fluorescence lifetimes were measured by a Horiba FluoroCube spectrofluorometer system with an Oxford Optistat DN for temperature control and a UV diode laser (NanoLED 375 nm).

Synthesis

2-(Anthracen-9-yl)acetonitrile (1).[25] The solution of 9-chloromethylanthracene (4.5 g, 19.9 mmol, 1 eq.) and NaCN (2.40g, 49.0 mmol, 2.5 eq.) in DMSO (68 mL) was stirred for 4 h at 55 °C under Ar atmosphere. After stirring for 4 h, the mixture was cooled to room temperature and diluted with 600 mL of water. Precipitation was collected by filtration and washed with H_2O. The pale yellow solid was obtained (4.26 g, 99%). ^{1}H NMR ($CDCl_3$): δ 8.52 (s, 1H), 8.18 (d, 2H, *J* = 8.8 Hz), 8.07 (d, 2H, *J* = 8.6 Hz), 7.64 (t, 2H, *J* = 7.8 Hz), 7.55 (t, 2H, *J* = 7.9 Hz), 4.60 (s, 2H). HRMS (ESI): *m/z* calcd. for $C_{16}H_{12}N$ ($M+H^+$): 218.0970. Found: 218.0970.

2-(Anthracen-9-yl)acetic acid (2).[25] KOH (1.15 g, 17.48 mmol, 4 eq.) in 10 mL of water was added to a suspension of 2-(anthracen-9-yl)acetonitrile (0.95 g, 4.37 mmol, 1 eq.) in ethylene glycol (50 mL). The mixture was refluxed for 24 h until generation of the homogenous solution. The hot solution was filtered, and the filtrate was acidified with dilute hydrochloric acid to obtain the precipitated product (0.91 g, 89%).

^{1}H NMR ($CDCl_3$): δ 8.44 (s, 1H), 8.24 (d, 2H, *J* = 8.8 Hz), 8.03 (d, 2H, *J* = 8.1 Hz), 7.54−7.45 (m, 4H), 4.65 (s, 2H). MS (EI): m/z 236 (M^+).

Protoporphyrin-IX DME (3).[26] Protoporphyrin-IX disodium salt (5.0 g, 8.24 mmol) was added to the stirred solution of the trimethyl orthoformate (250 mL) and MeOH (250 mL). Concentrated sulfuric acid (50 mL) was then added slowly, with cooling to room temperature, and the solution was stirred at room temperature for 2 h. The mixture was then diluted with water and neutralized with sat. $NaHCO_3$ aqueous solution. The mixture was extracted with CH_2Cl_2. The organic extracts were washed with water and dried over anhydrous Na_2SO_4. The solvent was removed under reduced pressure and the purple solid was dissolved in CH_2Cl_2 and reprecipitated in hexanes. The purple solid was obtained (4.31 g, 89%). ^{1}H NMR ($CDCl_3$): δ 10.11 (s, 2H), 9.98 (s, 2H) 8.23 (m, 2H), 6.36 (s, 1H), 6.32 (s, 1H), 6.18−6.15 (m, 2H), 4.36 (t, 4H, *J* = 6.8 Hz), 3.66 (m, 12H), 3.59 (m, 6H), 3.28 (t, 4H, *J* = 7.6 Hz) −3.83 (br, 2H). ^{13}C NMR ($CDCl_3$): δ 173.41, 130.22, 120.80, 98.06, 97.44, 97.13, 96.14, 51.75, 36.96, 30.95, 21.91, 12.78, 11.76. MS (MALDI): m/z 591 ($M+H^+$).

Mesoporphyrin-IX DME (4).[27] A two-neck-round-bottom flask was charged with the compound **3** (2.0 g, 3.38 mmol, 1 eq.), Pd/C (10% Pd, 60 mg), and DMF (250 mL), and the mixture was warmed to 60 °C with magnetic stirring under Ar atmosphere. Ammonium formate (3.20 g, 50.8 mmol, 15 eq.) was added to the reaction mixture. After stirring for 1.5 h, from the UV–vis spectrum of the sample mixture, complete conversion to mesoporphyrin-IX DME (**4**) was confirmed by the fact that the band at 630 nm attributable to the compound **3** was shifted to the band at 620 nm attributable to the compound **4**. The mixture was filtered through a celite. Water was added and the mixture was filtered. The obtained precipitate was dissolved in $CHCl_3$ and dried over anhydrous Na_2SO_4. The mixture was concentrated with a rotary evaporator to give a purple solid. The crude product was purified by silica gel column chromatography ($CHCl_3$ only). The purple solid was obtained (1.64 g, 81%). ^{1}H NMR ($CDCl_3$): δ 10.05 (s, 4H), 4.40 (m,

4H), 4.04 (m, 4H), 3.66–3.59 (m, 18H), 3.28 (m, 4H), 1.85 (t, 6H, J = 7.8 Hz), –3.81 (s, 2H). ^{13}C NMR ($CDCl_3$): δ 173.49, 96.57, 96.43, 96.18, 51.72, 37.07, 30.95, 21.99, 19.90, 17.74, 11.82, 11.78, 11.65, 11.61. HRMS (ESI): *m/z* calcd. for $C_{36}H_{43}N_4O_4$ ($M+H^+$): 595.3279. Found: 595.3267.

2,4-Diethyl-6,7-bis(3-hydroxypropyl)-1,3,5,8-tetramethylporphyrin (5).[28] The solution of meso-porphyrin-IX DME (1.4 g, 2.4 mmol, 1 eq.) and lithium aluminum hydride (0.90 g, 24 mmol, 10 eq.) in dry THF (140 mL) was stirred at room temperature for 1 h under Ar atmosphere. After stirring, the reaction was quenched with successive additions of water (0.9 mL), 15% aqueous sodium hydroxide (0.9 mL) and water (2.7 mL). The mixture was filtered through a celite and evaporated under reduced pressure. The residue was recrystallized with THF/MeOH. The purple crystals was obtained (0.70 g, 55%). ^{1}H NMR (DMSO-d_6): δ 10.27 (s, 1H), 10.19 (s, 1H), 10.17 (s, 2H), 4.20 (m, 4H), 4.11 (m, 4H), 3.99 (m, 4H), 3.64 (s, 12H), 2.52 (m, 4H), 2.36 (br, 2H) –3.76 (br, 2 H). HRMS (ESI): *m/z* calcd. for $C_{34}H_{43}N_4O_2$ ($M+H^+$): 539.3381. Found: 539.3381.

21H,23H-Porphine-2,18-dipropanol, 7,12-diethyl-3,8,13,17-tetramethyl-, bis(2-anthracen-9-yl) acetate (6). 2-(Anthracen-9-yl)acetic acid (**2**) (1.05 g, 4.45 mmol, 4 eq.) was added to thionyl chloride (8.0 mL, 13.0 g, 109.6 mmol), and the reaction mixture was stirred at room temperature under Ar atmosphere. The mixture was stirred for 2 h, and thionyl chloride was removed. The resultant residue was diluted with CH_2Cl_2 (20 mL) and was added to DMF (25 mL) containing the compound **5** (0.6 g, 1.11 mmol, 1 eq.) and Et_3N (1.6 mL, 1.16 g, 11.4 mmol, 10 eq.) dropwise at 0 °C. Then, the reaction mixture was stirred for 1 h at room temperature. The reaction mixture was filtrated, and the filtrate was concentrated under reduced pressure. The crude product was extracted with CH_2Cl_2 and sat. $NaHCO_3$ aqueous solution. Then, the organic layer was collected and dried over anhydrous Na_2SO_4. The solvent was removed under reduced pressure and the crude product was purified by silica gel column chromatography ($CHCl_3$ only). The crude product was reprecipitated with $CHCl_3$/hexane. The purple solid was obtained (0.81 g, 74%). ^{1}H NMR ($CDCl_3$): δ 10.04 (s, 1H), 9.96 (s 2H), 9.79 (s, 1H), 8.38 (s, 2H),

8.26 (m, 4H), 7.97 (s, 2H), 7.95 (s, 2H), 7.47–7.39 (m, 8H), 4.62 (d, 4H, *J* = 2.4 Hz), 4.33 (m, 4H), 4.06 (m, 4H), 3.83 (m, 4H), 3.60 (s, 6H), 3.20 (s, 6H), 2.43 (m, 4H), 1.84 (t, 6H, *J* = 7.6 Hz), –3.84 (br, 2H). ^{13}C NMR ($CDCl_3$): δ 171.3, 131.5, 130.5, 129.1, 127.3, 126.2, 126.1, 124.9, 124.3, 96.5, 96.5, 96.4, 96.6, 64.6, 34.3, 31.8, 22.7, 19.9, 17.7, 11.6, 11.6, 11.4, 11.3. HRMS (ESI): *m/z* calcd. for $C_{66}H_{62}N_4O_4$ (M^+): 974.47656. Found: 974.47524.

Platinum 21H,23H-porphine-2,18-dipropanol, 7,12-diethyl-3,8,13,17-tetramethyl-, bis(2-anthracen-9-yl) acetate (DA-PtP, 7). The compound **6** (0.30 g, 0.31 mmol, 1 eq.) and $Pt(acac)_2$ (0.36 g, 0.92 mmol, 3 eq.) were dissolved in benzonitrile (30 mL) and bubbled with N_2 for 10 min. The vessel was placed into the microwave cavity. Using a microwave power of 500 W, the reaction mixture was heated and stirred for 4 h under N_2 atmosphere. This procedure was repeated 3 times. After reaction, the vessel was removed from the microwave cavity and cooled to room temperature. The crude product was confirmed using UV–vis spectrophotometer and TLC. The solvent was removed under reduced pressure, and the crude product was purified by silica gel column chromatography ($CHCl_3$: hexane = 4: 1). After column chromatography, the crude product was recrystallized with $CHCl_3$/ MeOH. The red crystal was obtained (0.17 g, 47%). ^{1}H NMR($CDCl_3$): δ 9.90 (s, 1H), 9.84 (d, 2H, *J* = 4.4 Hz), 9.67 (s, 1H), 8.38 (s 2H), 8.26 (m, 4H), 7.97 (s, 2H), 7.95 (s, 2H), 7.48–7.39 (m, 8H), 4.57 (d, 4H, *J* = 4.8 Hz), 4.33 (m, 4H), 3.94 (m, 4H), 3.72 (q, 4H, *J* = 4.8 Hz), 3.49 (s, 6H), 3.15 (s, 6H), 2.40 (t, 4H, *J* = 6.4 Hz), 1.80 (t, 6H, *J* = 7.6 Hz). ^{13}C NMR ($CDCl_3$): δ 171.4, 141.5, 141.5, 139.6, 139.1, 138.7, 138.1, 138.1, 137.8, 135.4, 134.4, 131.6, 130.6, 129.2, 127.4, 126.2, 126.1, 125.0, 124.4, 99.2, 99.1, 98.4, 64.6, 34.2, 22.5, 19.7, 17.5, 11.4, 11.4, 11.2,11.1. HRMS (ESI): *m/z* calcd. for $C_{66}H_{60}N_4O_4Pt$ (M^+): 1167.42568. Found: 1167.42483.

Fluorescence measurements. As a stock solution, 1 mM sensitizer in THF and 1 mM anthracene in DMSO were prepared. By using the stock solution, various concentration samples dissolved in DMSO were prepared. Fluorescence measurements were executed at 25 °C with the excitation at 540 nm passing

through a 480 nm cut-off filter. Samples were bubbled with nitrogen for 1 h before the measurements. The quantum yields were determined by comparing to the fluorescence intensities in the spectra of anthracene with the excitation at 376 nm in DMSO according to Equation 3.

$$\Phi_{up} = \Phi_{(An,em,DMSO,376ex)} \cdot I_{up}/I_{(An,em,DMSO,376ex)} \cdot \varepsilon_{(An,376)}/\varepsilon_{(complex,540)} \cdot c_{An}/c_{complex} \cdot S_{1nm}/S_{15nm} \cdot E_{376}/E_{540} \quad (3)$$

Here, $\Phi_{(An,em,DMSO,376ex)}$ is the quantum yield of the fluorescence emission from anthracene with the excitation at 376 nm in DMSO determined to be 0.18 as an absolute value with an integrating sphere. I is the emission area calculated from the spectrum, ε is the molar extinct coefficient, c is the concentration, S is the light amplitude in each slit width, and E is the light amplitude in each wavelength.

To determine the quantum yields for each step, initially, we defined the quantum yield of upconversion (Φ_{up}) as Equation 4:

$$\Phi_{up} = \Phi_{ISC} \cdot \Phi_{sens} \cdot \Phi_{TTA} \cdot \Phi_{(An,em,DMSO,376ex)} \quad (4)$$

Here, the efficiency of the generation of the triplet-excited sensitizer (Φ_{ISC}) was approximately 0.9 according to the literature.[29] From the decrease of the emission band from the triplet-excited state of sensitizer, the efficiency for sensitizing (Φ_{sens}) was calculated according to Equation 5. The quantum yield of upconversion (Φ_{up}) was calculated as a relative value compared to the fluorescence emission of anthracene with the excitation at 376 nm. Thus, the efficiency of TTA (Φ_{TTA}) was obtained.

$$\Phi_{sens} = 1-(I/I_0) \quad (5)$$

Here, the integration of the phosphorescence from PtOEP was represented as I_0 in the absence and I in the presence of anthracene.

Results and Discussion

To improve TTA efficiency, accumulation of the triplet-excited emitters is essential.[23] By connecting emitters, improvement of upconversion efficiencies was observed.[30–34] Various assembly systems have been accomplished with good upconversion efficiencies[35–43] even in aqueous media by molecular assembling.[44–48] Moreover, by connecting the triplet sensitizer with aromatic units, the lifetime at the triplet-excited state can be efficiently elongated.[49] Indeed, it has been reported that the connection of a sensitizer and emitters is one of simple strategies.[50–56] Meanwhile, decrease in efficiency through energy transfer from the singlet-excited emitter to the sensitizer can potentially occur.[57] Based on these information, we designed the anthracene-tethered Pt-porphyrin complex (DA-PtP, Scheme 1) and compared the upconversion efficiency. Anthracene can work as an emitter in the TTA-supported upconversion system with the combination to PtOEP.[58] We presumed that the excitation energy of the Pt-porphyrin moiety in DA-PtP can immediately transfer to the anthracene moieties via the sensitizing reaction after excitation, followed by TTA to yield the singlet-excited anthracene. The synthetic route of DA-PtP is shown in Scheme 2. Each part was prepared according to the literatures.[25–29] The vinyl groups on the porphyrin ring formed the undesired complexes with Pt ions, resulting in the generation of insoluble solids. To inhibit the complexation at the vinyl groups, the hydration carried out yielding ethyl groups. The metallation of the porphyrin was executed under microwave irradiation for 24 h. The resulting product showed good solubility in tetrahydrofuran (THF) and chloroform (several mM) and moderate solubility in DMSO (several ten μM). In addition, less significant degradation of the porphyrin ring was observed after the reaction.

Scheme 2

Initially, we compared the upconversion properties of the solution containing anthracene in the presence of PtOEP and DA-PtP in DMSO. The TTA process of photon upconversion is illustrated in Scheme 1.[23,58] Pt-porphyrin complexes can be a photosensitizer for exciting anthracene to the triplet-excited state by the

light irradiation at 540 nm, and subsequently singlet-excited anthracene can be generated from two triplet-excited anthracene via TTA. As a result, fluorescence emission from anthracene can be obtained. Photoluminescence was measured with the solution containing 100 μM anthracene and variable concentrations of the sensitizers in DMSO with an excitation at 540 nm with a 480 nm cut-off filter to eliminate the direct excitation of anthracene by a half wavelength light generated inevitably from xenon lamps. The typical fluorescence spectra with the vibration structures in anthracene were observed (Figures 1a, 1b and S1). Notably, by reducing the concentration of PtOEP to 5 μM, the emission band at the shortest wavelength around 410 nm disappeared (Figure 1c). On the other hand, in the presence of DA-PtP, the fluorescence emission with the peak at 410 nm remained even at 5 μM concentration of DA-PtP. This result means that DA-PtP has the ability to generate higher-energy photons than PtOEP. Same experiments were performed by changing the anthracene concentrations (Figures 1d and S2). Apparently, the significant emission band around 410 nm can be detected even by decreasing the emitter concentration to 50 μM. These data clearly indicate that DA-PtP can cause the photon upconversion to higher energy levels than PtOEP under diluted conditions.

Figure 1

From the UV–vis absorption spectra of the sensitizers, the similar Soret and Q bands to PtOEP were observed from DA-PtP, indicating that electronic structures of both porphyrin complexes should be almost same (Figure S3). Therefore, we assumed that the quantum yields of the triplet-excited state of DA-PtP could be similar to that of PtOEP. To estimate differences in electronic properties between the anthracene moieties in DA-PtP and free anthracene, the emission spectrum of 2-(anthracen-9-yl)acetic acid (**2**), which is considered to be equivalent to that of anthracene moiety of DA-PtP, was compared to that of anthracene (Figure 2). The red shifted emission was observed from **2**, and peak positions were not fitted to those of the upconversion emission. From the mixture containing DA-PtP and anthracene, the emission bands from DA-PtP were also measured with the excitation lights at 350 nm and 540 nm, respectively. Both of subtle

emissions assigned as fluorescence from the anthracene moieties and phosphorescence from the Pt complex were obtained. The efficient energy transfers from the triplet-excited Pt-porphyrin complex to anthracene and the single-excited anthracene to the Pt-porphyrin complex should occur. These results suggest the significant issue. The most of emission via the TTA-supported upconversion from the mixture solutions containing DA-PtP and anthracene should be not from the anthracene moiety in DA-PtP but from the free anthracene in the solution. The triplet-excited state should be immediately transported to the free anthracene via the anthracene moieties of DA-PtP, followed by the TTA-supported upconversion.

Figure 2

We calculated the efficiencies and quantum yields of each step to the emission as a relative value (Table 1). Here, we defined the quantum yield of upconversion (Φ_{up}) as the equation 1:

$$\Phi_{up} = \Phi_{ISC} \cdot \Phi_{sens} \cdot \Phi_{TTA} \cdot \Phi_{An,em} \qquad (1)$$

The quantum yield of fluorescence emission from anthracene ($\Phi_{An,em}$) was determined to be 0.18 as an absolute value with an integrating sphere. According to the above results, the efficiencies of the generation of the triplet-excited Pt-porphyrin complexes were approximately 0.9.[29] From the decreases in the emission bands of the triplet-excited state of PtOEP and DA-PtP observed between 600–750 nm by the addition of anthracene, the efficiencies for sensitizing (Φ_{sens}) were determined as 0.736 and 0.831, respectively. Quantum yields of upconversion (Φ_{up}) in the presence of PtOEP and DA-PtP were calculated to be 0.00345 and 0.00303 as a relative value compared to the fluorescence emission of anthracene with the excitation at 376 nm.[23] Thus, the efficiencies of TTA (Φ_{TTA}) with PtOEP and DA-PtP were obtained as 0.00291 and 0.00234, respectively. These data indicate that similar efficiencies were obtained in each

step from both processes. In other words, without loss of efficiencies, DA-PtP can generate higher-energy photons.

Table 1

To gather information for the reason why the higher energy photon can be generated from the solution containing DA-PtP although electronic properties were almost same to PtOEP, we carried out the further experiments. We hypothesized that Pt-porphyrin complexes and anthracene could agglomerate via the stacking due to the planar structures and high lipophilicity. These static interactions in the solution states might cause the decay of the higher-energy photons. This assumption was able to be significantly supported by the results from the Stern–Volmer plots of the phosphorescence of the sensitizers with anthracene (Figure 3).[59] By increasing the concentration of anthracene, decrease in intensity of phosphorescence from the Pt porphyrin moiety was observed from the sample containing An-PtP. The linear relationship was obtained from the Stern–Volmer plots through the detection concentration range. On the other hand, the slope of the line was relatively-small of the sample containing PtOEP. In particular, the quenching effect by adding anthracene reached a plateau in the presence of 50 μM of anthracene, indicating that the static interaction between PtOEP and anthracene should be formed. The agglomeration of anthracene to PtOEP could occur due to high hydrophobicity and planarity. We were able to determine the lifetimes of the phosphorescence with the single component from the samples because of enough emission intensity for the evaluations (Table 1). Accordingly, two significant features were observed. First, lifetimes were shortened by adding anthracene, clearly indicating that energy transfer to free anthracene molecules should occur from both sensitizers. Second, longer lifetimes were observed from the samples containing DA-PtP in the presence and absence of anthracene, comparing to those of PtOEP. This result supports the fact that PtOEP could form larger degree of aggregation where emission annihilation should be critically induced by concentration quenching. Thus, to realize shorter-wavelength

light through TTA-supported upconversion, it should be essential to suppress aggregation of the sensitizers.

Figure 3

According to the experimental data, we assumed the plausible models to explain the differences in the upconversion behaviors. Around PtOEP, molecular agglomeration with anthracene could be formed, and the series of the photochemical processes take place mainly within agglomeration. Thereby, reabsorption of higher-energy photons should readily proceed. In contrast, formation of agglomeration can be effectively disturbed by DA-PtP. Furthermore, transmittance of excitation energy to free anthracenes was encouraged by the dual-anthracene substituents. Thus, higher-energy photons can be preserved from reabsorption by the Pt complex. In this study, we mainly focus on not efficiency but energy levels of the converted photon. Porphyrin complexes are one of the effective sensitizers for presenting TTA-supported upconversion with low-power incident light.[17,58,60–63] It is assumed that agglomeration around the sensitizer, followed by enhancing local concentrations could contribute to improving upconversion efficiencies.

CONCLUSION

We describe here the upconversion for generating higher-energy photons under diluted conditions by utilizing the novel sensitizer, DA-PtP. From the series of the experiments, it was implied that the two anthracene molecules tethered to the Pt-porphyrin complex could play significant roles in presenting the higher-energy photons not only by mediating the excited energy from the Pt-porphyrin complex to the free anthracene but also by inhibiting the agglomeration of anthracene and subsequently reabsorption to the Pt complex. Our system is composed of combination with conventional molecules such as PtOEP and anthracene. This means that further improvement of efficiencies in each step and tuning of wavelengths

of the incident light and emission could be feasible by replacing the specialized molecules. Thus, this concept might be valid for enhancing upconversion efficiencies in the other established systems.

ACKNOWLEDGEMENT

This work was partially supported by the Kato Memorial Bioscience Foundation (for K.T.) and a Grant-in-Aid for Scientific Research on Innovative Areas “New Polymeric Materials Based on Element-Blocks (No.2401)” (JSPS KAKENHI Grant Number JP24102013).

REFERENCES

1. Ito T, Tanabe K, Yamada H, Hatta H, Nishimoto S. Radiation- and Photo-induced Activation of 5-Fluorouracil Prodrugs as a Strategy for the Selective Treatment of Solid Tumors. Molecules 2008;13:2370−84.

2. Photochemical and Photodynamical Properties of Sulfur-Substituted Nucleic Acid Bases. Photochem Photobiol 2019;95:33−58.

3. Imran M, Ayub W, Butler IS, Rehman Z. Photoactivated platinum-based anticancer drugs. Coordin Chem Rev 2018;376:405−29.

4. Huan L et al. Expanding Anti-Stokes Shifting in Triplet–Triplet Annihilation Upconversion for In Vivo Anticancer Prodrug Activation. Angew Chem Int Ed 2017;56:14400−4.

5. Kerzig C, Wenger OS. Sensitized triplet–triplet annihilation upconversion in water and its application to photochemical transformations. Chem Sci 2018;9:6670−8.

6. Manna MK et al. New perspectives for triplet–triplet annihilation based photon upconversion using all-organic energy donor & acceptor chromophores. Chem Commun 2018;54:5809−18.

7. Singh-Rachford TN, Castellano FN. Photon upconversion based on sensitized triplet–triplet annihilation. Coord Chem Rev 2010;254:2560−73.

8. Bharmoria P, Yanai N, Kimizuka N. Recent Progress in Photon Upconverting Gels. Gels 2019;5:18.

9. Gray V et al. Towards efficient solid-state triplet–triplet annihilation based photon upconversion: Supramolecular, macromolecular and self-assembled systems. Coord Chem Rev 2018;362:54−71.

10. Dou Q et al. Bioimaging and biotedection assisted with TTA-UC materials. Drug Discov Today 2017;22:1400−11.

11. Askes SHC et al. Imaging Upconverting Polymersomes in Cancer Cells: Biocompatible Antioxidants Brighten Triplet–Triplet Annihilation Upconversion. Small 2016;12:5579−90.

12. Xu M et al. Ratiometric nanothermometer in vivo based on triplet sensitized upconversion. Nat Chem 2018;9:2698.

13. Park J, Xu M, Li F, Zhou H-C. 3D Long-Range Triplet Migration in a Water-Stable Metal–Organic Framework for Upconversion-Based Ultralow-Power in Vivo Imaging. J Am Chem Soc 2018;140:5493−9.

14. Tian B et al. In vivo biodistribution and toxicity assessment of triplet-triplet annihilation-based upconversion nanocapsules. Biomaterials 2017;112:10−19.

15. Liu Q et al. Highly Photostable Near-IR-Excitation Upconversion Nanocapsules Based on Triplet−Triplet Annihilation for in Vivo Bioimaging Application. ACS Appl Mater Informatics 2018;10:9883−8.

16. Liu Q et al. A General Strategy for Biocompatible, High-Effective Upconversion Nanocapsules Based on Triplet−Triplet Annihilation. J Am Chem Soc 2013;135:5029−37.

17. Singh-Rachford TN, Castellano FN, Low Power Visible-to-UV Upconversion. J Phys Chem 2009;113:5912−7.

18. Yanai N, Kozue M, Amemori S, Kabe R, Adachi C, Kimizuka N. Increased vis-to-UV upconversion performance by energy level matching between a TADF donor and high triplet energy acceptors. J Mater Chem C 2016;4:6447−51.

19. Barawi M et al. Photoelectrochemical Hydrogen Evolution Driven by Visible-to-Ultraviolet Photon Upconversion. ACS Appl Energy Mater 2019;2:207−11.

20. Deng F, Blumhoff J, Castellano FN. Annihilation Limit of a Visible-to-UV Photon Upconversion Composition Ascertained from Transient Absorption Kinetics. J Phys Chem A 2013;117:4412−9.

21. Gon M, Tanaka K, Chujo Y. Recent Progress in the Development of Advanced Element-Block Materials. Polym J 2018;50:109−26.

22. Chujo Y, Tanaka K. New Polymeric Materials Based on Element-Blocks. Bull Chem Soc Jpn 2015;88:633−43.

23. Tanaka K et al. Environment-Responsive Upconversion Based on Dendrimer-Supported Efficient Triplet-Triplet Annihilation in Aqueous Media. Chem Commun 2010;46:4378–80.

24. Tanaka K et al. Hypoxic Conditions-Selective Upconversion via Triplet-Triplet Annihilation Based on POSS-Core Dendrimer Complexes. Bioorg Med Chem 2013;21:2678–81.

25. Shah JR et al. Synthesis, structure–affinity relationships, and modeling of AMDA analogs at 5-HT_{2A} and H_1 receptors: Structural factors contributing to selectivity. Bioorg Med Chem 2009;17: 6496−504.

26. Byrne CJ, Ward AD. A facile porphyrin esterification/etherification procedure. Tetrahedron Lett 1988;29:1421–4.

27. Rebouças JS, James BR. A simple, catalytic H2-hydrogenation method for the synthesis of fine chemicals; hydrogenation of protoporphyrin IX dimethyl ester. Tetrahedron Lett 2006;47:5119–22.

28. Burns DH, Lai J-J, Smith KM. Syntheses of chlorins from unsymmetrically substituted iron porphyrins. J Chem Soc Perkin Trans 1988;1:3119–31.

29. Kavandi J et al. Luminescent barometry in wind tunnels. Rev Sci Instrum 1990;61:3340–7.

30. Ogawa T, Yanai N, Fujiwara S, Nguyen T-Q, Kimizuka N. Aggregation-free sensitizer dispersion in rigid ionic crystals for efficient solid-state photon upconversion and demonstration of defect effects. J Mater Chem C 2018;6:5609−15.

31. Chidanguro T et al. Fabrication of single-chain nanoparticles through the dimerization of pendant anthracene groups via photochemical upconversion. Dalton Trans 2018;47:8663−9.

32. Lee SH et al. Light upconversion by triplet–triplet annihilation in diphenylanthracene-based copolymers. Polym Chem 2014;5:6898–904.

33. Yu X et al. Triplet–triplet annihilation upconversion from rationally designed polymeric emitters with tunable inter-chromophore distances. Chem Commun 2015;51:588–91.

34. Dzebo D et al. Intramolecular Triplet−Triplet Annihilation Upconversion in 9,10-Diphenylanthracene Oligomers and Dendrimers. J Phys Chem C 2016;120:23397–406.

35. Yanai N, Kimizuka N. Recent emergence of photon upconversion based on triplet energy migration in molecular assemblies. Chem Commun 2016;52:5354−84.

36. Kimizuka N, Yanai N, Morikawa M. Photon Upconversion and Molecular Solar Energy Storage by Maximizing the Potential of Molecular Self-Assembly. Langmuir 2016;32:12304−22.

37. Hisamitsu S, Yanai N, Kimizuka N. Photon-Upconverting Ionic Liquids: Effective Triplet Energy Migration in Contiguous Ionic Chromophore Arrays. Angew Chem Int Ed 2015;54:11550−4.

38. Gray V et al. Singlet and triplet energy transfer dynamics in self-assembled axial porphyrin–anthracene complexes: towards supra-molecular structures for photon upconversion. Phys Chem Chem Phys 2018;20:7549−58.

39. Fan C et al. Enhanced Triplet − Triplet Energy Transfer and Upconversion Fluorescence through Host − Guest Complexation. J Am Chem Soc 2016;138:15405−12.

40. Hisamitsu S, Yanai N, Kouno H, Magome E, Matsuki M, Yamada T, Monguzzi A, Kimizuka N. Two-dimensional structural ordering in a chromophoric ionic liquid for triplet energy migration-based photon upconversion. Phys Chem Chem Phys 2018;20:3233−40.

41. Goudarzi H, Keivanidis PE. All-Solution-Based Aggregation Control in Solid-State Photon Upconverting Organic Model Composites. ACS Appl Mater Interfaces 2017;9:845−57.

42. Zhou Y et al. Examining the role of acceptor molecule structure in self-assembled bilayers: surface loading, stability, energy transfer, and upconverted emission. Phys Chem Chem Phys 2018;20:20513−24.

43. Dilbech T, Hill SP, Hanson K. Harnessing molecular photon upconversion at sub-solar irradiance using dual sensitized self-assembled trilayers. J Mater Chem A 2017;5:11652−60.

44. Bharmoria P, Hisamitsu S, Nagatomi H, Ogawa T, Morikawa M, Yanai N, Kimizuka N. Simple and Versatile Platform for Air-Tolerant Photon Upconverting Hydrogels by Biopolymer−Surfactant−Chromophore Co-assembly. J Am Chem Soc 2018;140:10848−55.

45. Haruki R, Kouno H, Hosoyamada M, Ogawa T, Yanai N, Kimizuka N. Oligo(ethylene glycol)/alkyl-modified Chromophore Assemblies for Photon Upconversion in Water. Chem Asian J 2019;14:1723−8.

46. Kouno H, Sasaki Y, Yanai N, Kimizuka N. Supramolecular Crowding Can Avoid Oxygen Quenching of Photon Upconversion in Water Chem Eur J 2019;25:6124−30.

47. Xu W et al. Supramolecular Assembly-Improved Triplet–Triplet Annihilation Upconversion in Aqueous Solution. Chem Eur J 2018;24:16677−85.

48. Kouno H, Ogawa T, Amemori S, Mahato P, Yanai N, Kimizuka N. Triplet energy migration-based photon upconversion by amphiphilic molecular assemblies in aerated water. Chem Sci 2016;7:5224−9.

49. Cui X, Zhao J, Mohmood Z, Zhang C. Accessing the Long-Lived Triplet Excited States in Transition-Metal Complexes: Molecular Design Rationales and Applications. Chem Rec 2016;16:173–188.

50. Guo X et al. New Bichromophoric Triplet Photosensitizer Designs and Their Application in Triplet–Triplet Annihilation Upconversion. Adv Optical Mater 2018;6:1700981.

51. Deng F, Lazorski MS, Castellano. Photon upconversion sensitized by a Ru(II)-pyrenyl chromophore. Phil Trans R Soc A 2015;373:20140322.

52. Wang Z et al. Increasing the anti-Stokes shift in TTA upconversion with photosensitizers showing red-shifted spin-allowed charge transfer absorption but a non-compromised triplet state energy level. Chem Commun 2019;50:1510−3.

53. Lee SH et al. Glassy Poly(methacrylate) Terpolymers with Covalently Attached Emitters and Sensitizers for Low-Power Light Upconversion. J Polym Sci A: Polym Chem 2015;53:1629–39.

54. Xu K, Zhao J, Moore EG. Covalently Bonded Perylene−DiiodoBodipy Dyads for Thiol-Activatable Triplet−Triplet Annihilation Upconversion. J Phys Chem C 2017;121:22665–79.

55. Boutin PC et al. Photon Upconversion by Triplet−Triplet Annihilation in Ru(bpy) 3- and DPA-Functionalized Polymers. J Phys Chem Lett 2013;4:4113−4118.

56. Porphyrin−Anthracene Complexes: Potential in Triplet−Triplet Annihilation Upconversion. J Phys Chem C 2016;120:19018−19026.

57. Kozlov DV, Castellano FN. Anti-Stokes delayed fluorescence from metal–organic bichromophores. Chem Commun 2004:2860−1.

58. Islangulov RR, Lott J, Weder C, Castellano FN. Noncoherent Low-Power Upconversion in Solid Polymer Films. J Am Chem Soc 2007;129:12652−3.

59. Sugunan SK et al. Mechanisms of Low-Power Noncoherent Photon Upconversion in Metalloporphyrin - Organic Blue Emitter Systems in Solution. J Phys Chem A 2009;113:8548−56.

60. Singh-Rachford TN, Lott J, Weder C, Castellano FN. Influence of Temperature on Low-Power Upconversion in Rubbery Polymer Blends. J Am Chem Soc 2009;131:12007−14.

61. Islangulov RR, Kozlov DV, Castellano FN. Low power upconversion using MLCT sensitizers. Chem Commun 2005:3776−8.

62. Baluschev S et al. Up-Conversion Fluorescence: Noncoherent Excitation by Sunlight. Phys Rev Lett 2006;97:143903.

63. Singh-Rachford TN, Haefele A, Ziessel R, Castellano FN. Boron Dipyrromethene Chromophores: Next Generation Triplet Acceptors/Annihilators for Low Power Upconversion Schemes. J Am Chem Soc 2008;130:16164−5.

TABLE AND FIGURES

Scheme 1. Schematic model of the TTA-supported upconversion and chemical structures of the sensitizers used in this study

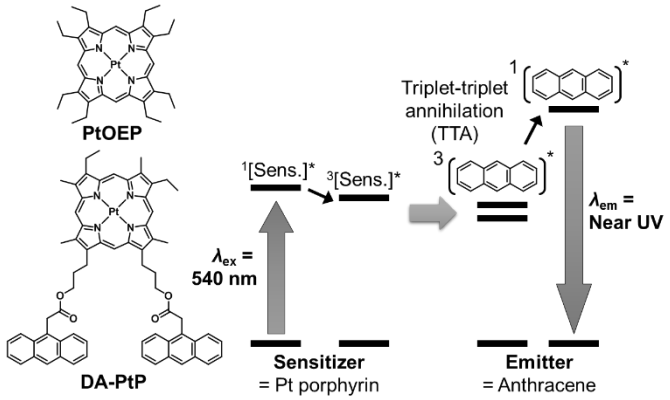

Scheme 2. Synthesis of DA-PtP[a]

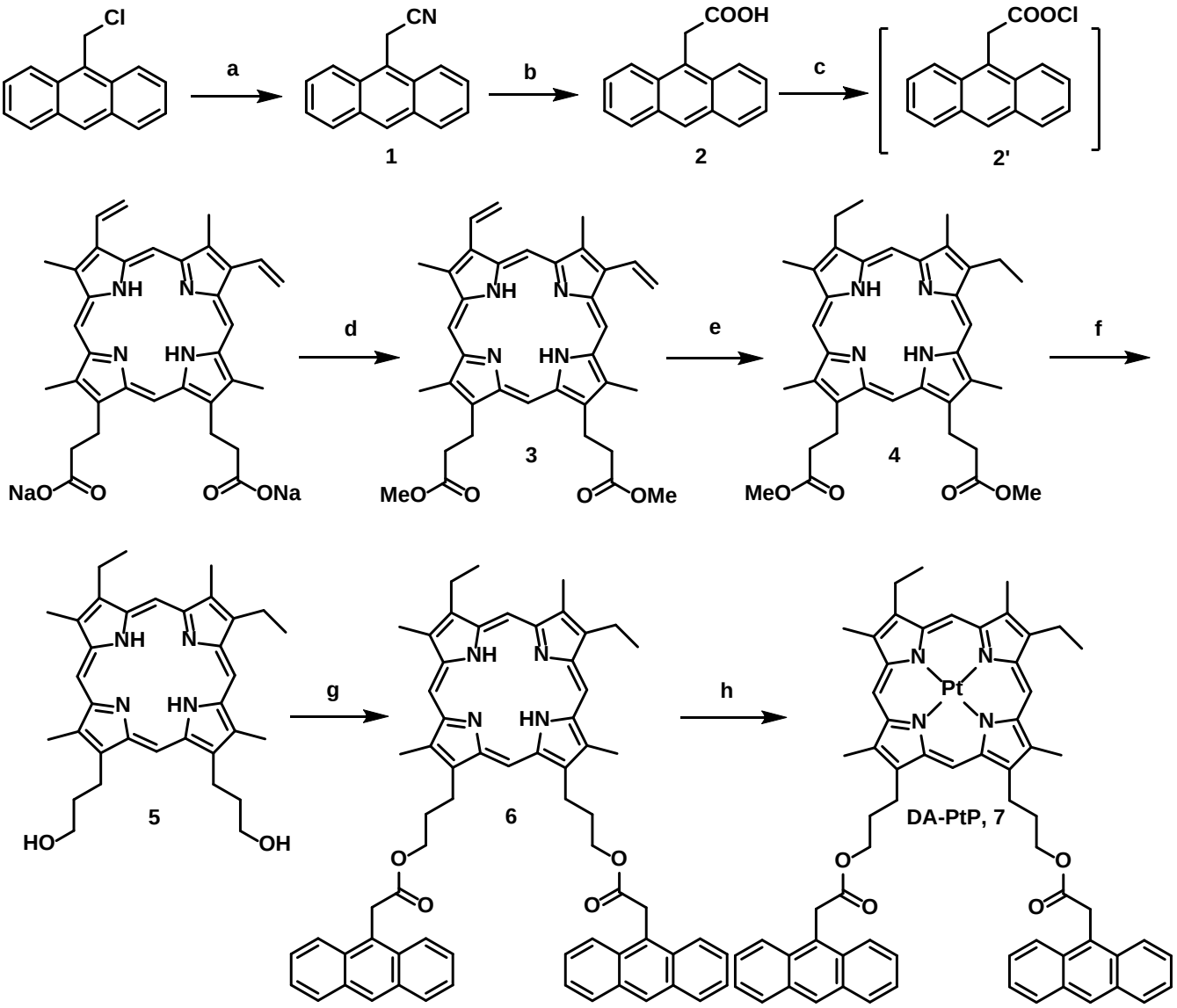

[a]Reagents and condition: a) NaCN, DMSO, 55 °C, 4 h, 99%; b) KOH, H_2O/ethylene glycol, reflux, 24 h, 89%; c) $SOCl_2$, r.t., 1 h; d) MeOH, $(CH_3)_3CH$, H_2SO_4, r.t., 2 h, 89%; e) NH_4COOH, Pd/C, DMF, 60 °C, 1.5 h, 81%; f) LAH, THF, 1 h, 55%; g) 2', NEt_3N, CH_2Cl_2/DMF, 0 °C to r.t., 74%; h) $Pt(acac)_2$, benzonitrile, Microwave 500 W, 12 h, 47%.

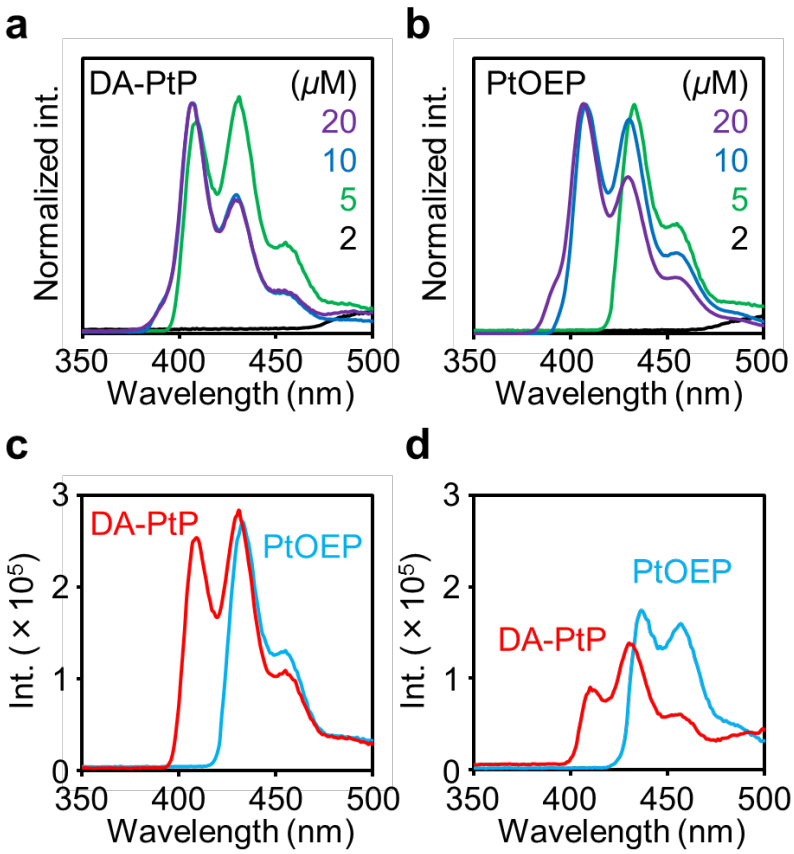

Figure 1. Fluorescence spectra of the samples containing 100 μM anthracene and variable concentrations of (a) DA-PtP and (b) PtOEP and (c) 5 μM sensitizer and (d) 50 μM anthracene and 5 μM sensitizer in DMSO with the excitation at 540 nm passing through a 480 nm cut-off filter.

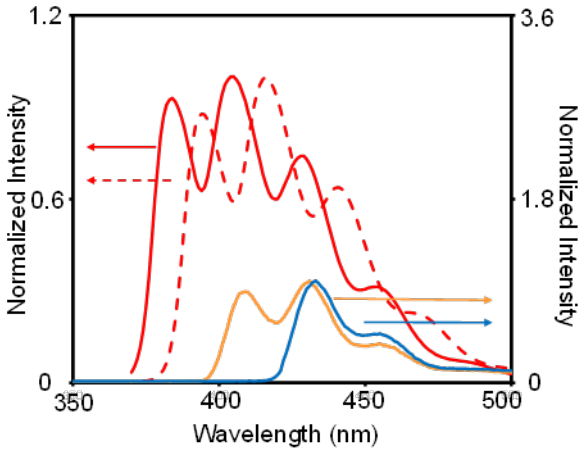

Figure 2. Fluorescence spectra of the samples containing 100 μM anthracene (red line) and 100μM compound **2** (red dashed line) in DMSO with the excitation at absorption maxima. Fluorescence spectra via TTA of the samples containing 5 μM PtOEP and 100 μM anthracene (blue line) and 5 μM DA-PtP and 100 μM anthracene (orange line) in DMSO with the excitation at 540 nm passing through a 480 nm cut-off filter.

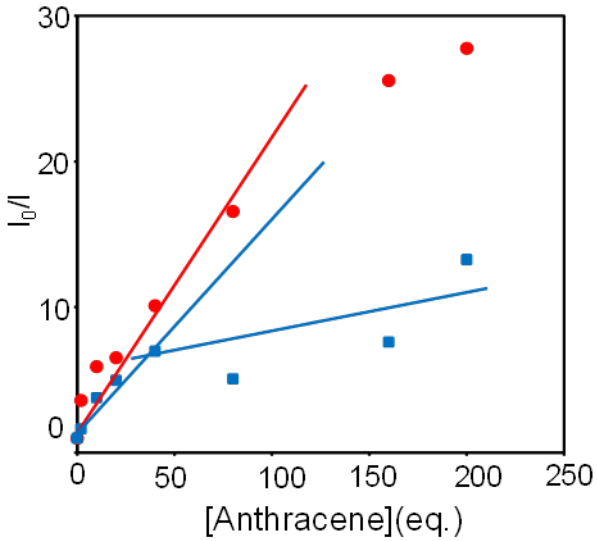

Figure 3. Stern–Volmer plots of the phosphorescence of PtOEP (blue plots) and DA-PtP (red plots) with anthracene.

Table 1. Optical properties in the TTA-supported upconversion[a]

sensitizer	Φ_{ISC}	Φ_{sens}	Φ_{TTA}	Φ_{up} ($\times 10^{-3}$)	τ (ns)[b]	τ (ns)[b,c]
DA-PtP	0.9	0.831	0.00234	0.303	729	634
PtOEP	0.9	0.733	0.00291	0.334	612	538

[a]Determined with 5 μM sensitizer and 100 μM anthracene in DMSO.
[b]5 μM sensitizer in DMSO with the excitation light at 375 nm (detection wavelength at 540 nm).
[c]In the presence of 100 μM anthracene.

GRAPHICAL ABSTRACT

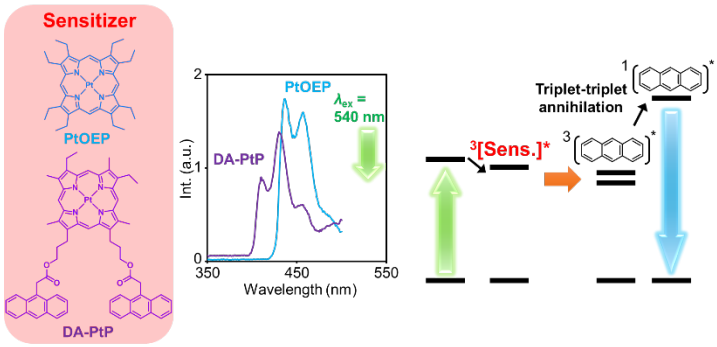

Supporting Information

Development of the Sensitizer for Generating Higher-Energy Photons under Diluted Condition via the Triplet-Triplet Annihilation-Supported Upconversion

Kazuo Tanaka, Wataru Ohashi, Kenichi Inafuku, Shohei Shiotsu, Yoshiki Chujo*

Department of Polymer Chemistry, Graduate School of Engineering, Kyoto University,

Katsura, Nishikyo-ku, Kyoto 615-8510, Japan

E-mail: tanaka@poly.synchem.kyoto-u.ac.jp

Phone: +81-75-383-2604

Fax: +81-75-383-2605

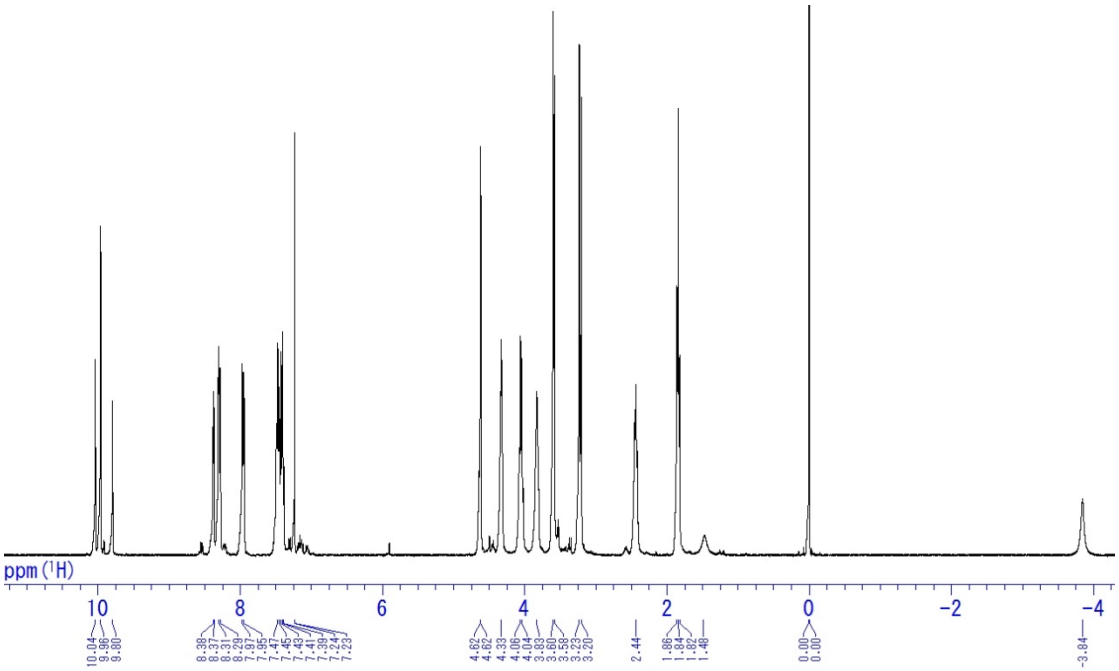

Chart S1. ^{1}H NMR spectrum of **6** in $CDCl_3$.

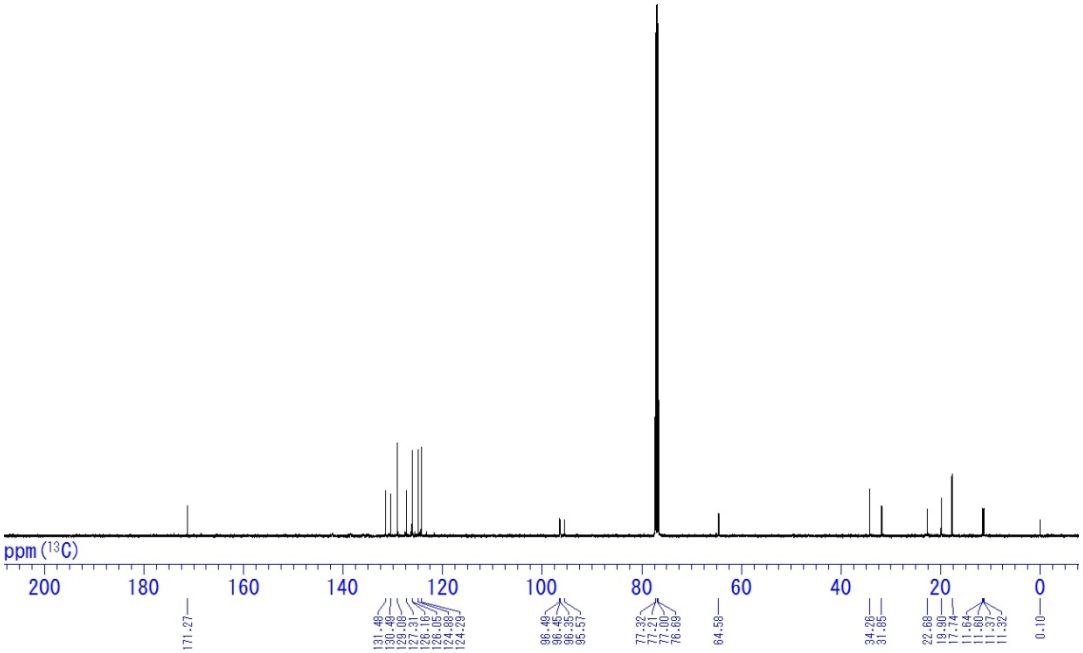

Chart S2. ^{13}C NMR spectrum of **6** in $CDCl_3$.

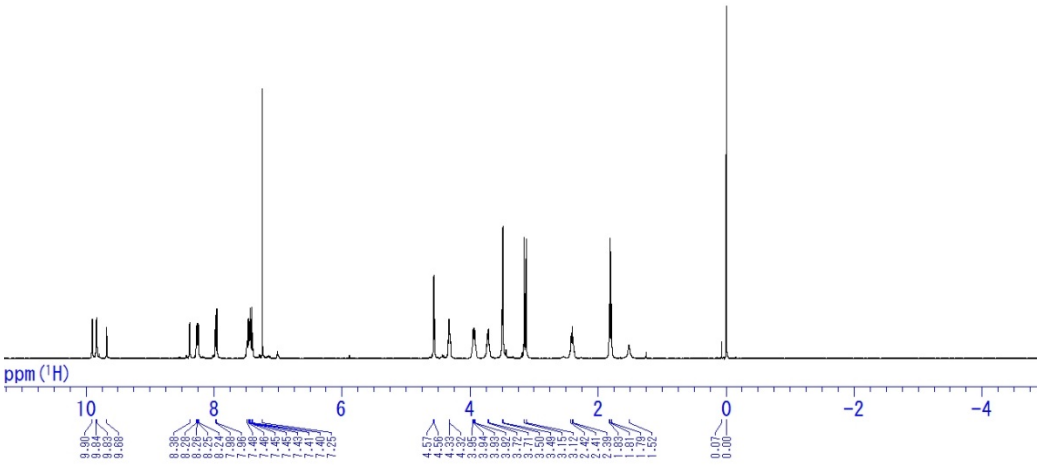

Chart S3. ^{1}H NMR spectrum of **DA-PtP** in $CDCl_3$.

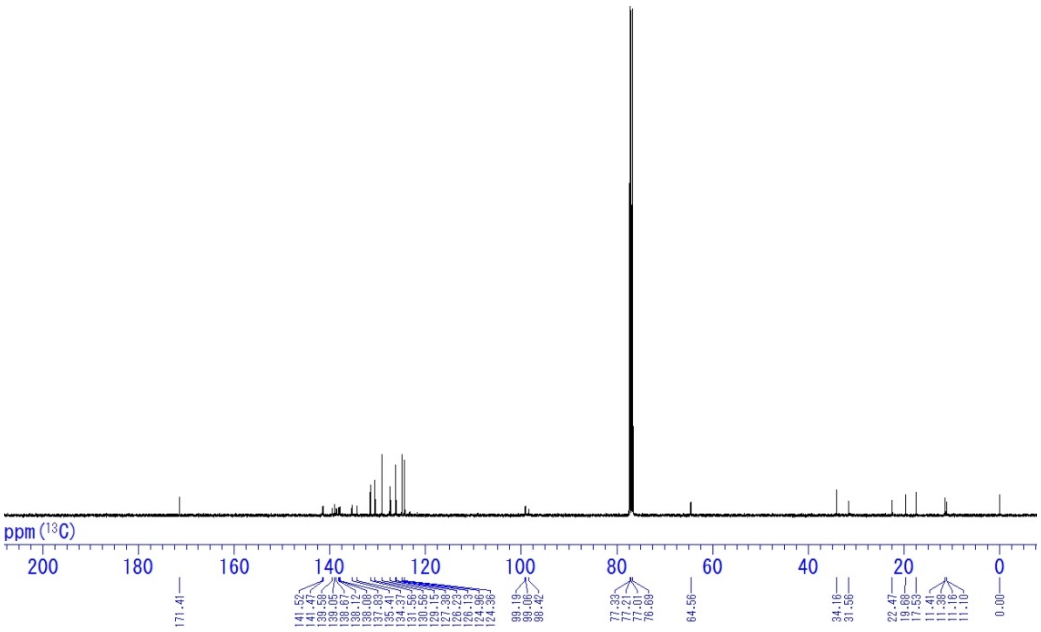

Chart S4. ^{13}C NMR spectrum of **DA-PtP** in $CDCl_3$.

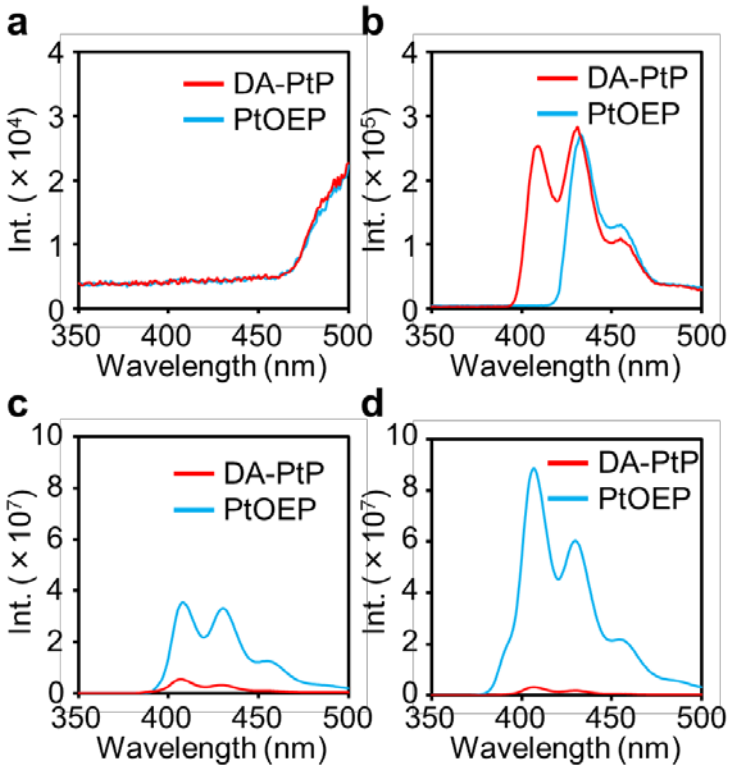

Figure S1. Fluorescence spectra of the samples containing 100 μM anthracene and various concentrations of sensitizers (a: 2 μM, b: 5 μM, c: 10 μM, d: 20 μM) in DMSO with the excitation at 540 nm passing through a 480 nm cut-off filter.

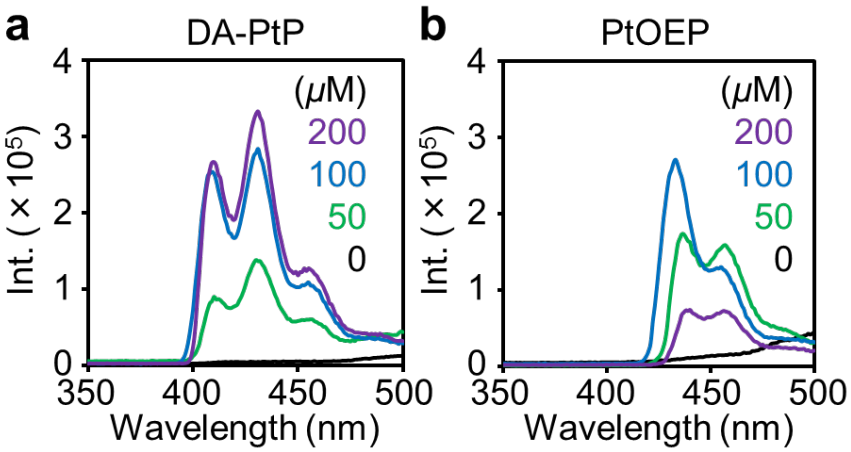

Figure S2. Fluorescence spectra of the samples containing various concentrations of anthracene and 5 μM sensitizer in DMSO with the excitation at 540 nm passing through a 480 nm cut-off filter.

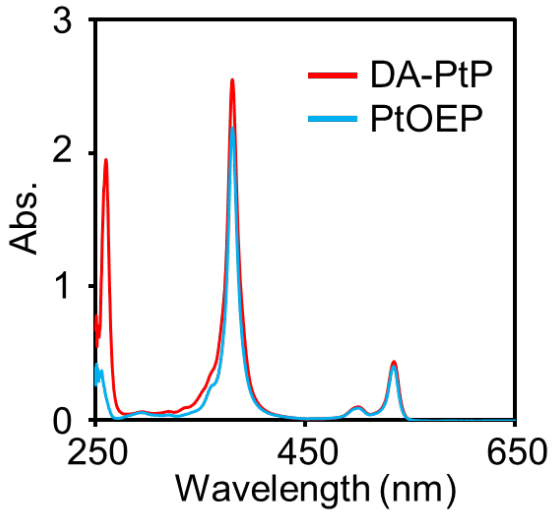

Figure S3. (a) UV−vis absorption spectra of DA-PtP and PtOEP in DMSO (5 μM).